

Edited by
Landong Li and Justin S. J. Hargreaves

Heterogeneous Catalysis for Sustainable Energy



Heterogeneous Catalysis for Sustainable Energy

Heterogeneous Catalysis for Sustainable Energy

Edited by Landong Li and Justin S. J. Hargreaves

WILEY-VCH

Editors

Prof. Landong Li

Nankai University
School of Materials Science and
Engineering
38# Tongyan Road
Haihe Education Park
Jinnan District
300350 Tianjin
China

Prof. Justin S. J. Hargreaves

University of Glasgow
School of Chemistry
Joseph Black Building
G12 8QQ Glasgow
United Kingdom

Cover Image: © skegbydave/Getty Images

■ All books published by **WILEY-VCH** are carefully produced. Nevertheless, authors, editors, and publisher do not warrant the information contained in these books, including this book, to be free of errors. Readers are advised to keep in mind that statements, data, illustrations, procedural details or other items may inadvertently be inaccurate.

Library of Congress Card No.: applied for

British Library Cataloguing-in-Publication Data

A catalogue record for this book is available from the British Library.

Bibliographic information published by the

Deutsche Nationalbibliothek The Deutsche Nationalbibliothek lists this publication in the Deutsche Nationalbibliografie; detailed bibliographic data are available on the Internet at <<http://dnb.d-nb.de>>.

© 2022 WILEY-VCH GmbH, Boschstr. 12,
69469 Weinheim, Germany

All rights reserved (including those of translation into other languages). No part of this book may be reproduced in any form – by photoprinting, microfilm, or any other means – nor transmitted or translated into a machine language without written permission from the publishers. Registered names, trademarks, etc. used in this book, even when not specifically marked as such, are not to be considered unprotected by law.

Print ISBN: 978-3-527-34485-7

ePDF ISBN: 978-3-527-81589-0

ePub ISBN: 978-3-527-81591-3

oBook ISBN: 978-3-527-81590-6

Typesetting Straive, Chennai, India

Printed on acid-free paper

10 9 8 7 6 5 4 3 2 1

Contents

Preface *xiii*

Part I Hydrogen Economy 1

- 1 Catalytic Hydrogen Production** 3
Xingyuan Gao and Sibudjing Kawi
- 1.1 Introduction 3
- 1.1.1 Thermocatalytic Decomposition of Methane 3
- 1.1.1.1 Metal Catalysts 4
- 1.1.1.2 Carbon Catalysts 5
- 1.1.2 Partial Oxidation of Methane 5
- 1.1.3 Catalytic Reforming of Methane 9
- 1.1.3.1 Steam Reforming of Methane (SRM) 9
- 1.1.3.2 Oxidative Steam Reforming of Methane (OSRM) 13
- 1.1.3.3 CO₂/Dry Reforming of Methane 14
- 1.1.4 Thermocatalytic Conversion of Other Fossil Fuels 21
- 1.2 Conclusions and Prospects 25
- References 25
- 2 Catalytic Reforming of Oxygen-Containing Chemicals** 33
Wei Luo, Song Song, Tong Ding, Ye Tian, and Xingang Li
- 2.1 Introduction 33
- 2.2 Catalytic Hydrogen Production from Methanol 33
- 2.2.1 Catalytic Hydrogen Production from Decomposition of Methanol 34
- 2.2.2 Catalytic Hydrogen Production from Partial Oxidation of Methanol 35
- 2.2.3 Catalytic Hydrogen Production from Steam Reforming of Methanol 36
- 2.2.4 Catalytic Hydrogen Production from Combined Reforming of Methanol 37
- 2.2.5 Catalytic Hydrogen Production from Aqueous-Phase Reforming of Methanol 37
- 2.3 Catalytic Hydrogen Production from Ethanol 38
- 2.3.1 Catalytic Hydrogen Production from Steam Reforming of Ethanol 39

2.3.2	Catalytic Hydrogen Production from Aqueous-Phase Reforming of Ethanol	41
2.4	Catalytic Hydrogen Production from Dimethyl Ether	42
2.4.1	Catalytic Hydrogen Production from Partial Oxidation of Dimethyl Ether	42
2.4.2	Catalytic Hydrogen Production from Autothermal Reforming of Dimethyl Ether	43
2.4.3	Catalytic Hydrogen Production from Steam Reforming of Dimethyl Ether	43
2.4.3.1	Mixed Bifunctional Catalysts	44
2.4.3.2	Supported Bifunctional Catalysts	44
2.5	Catalytic Hydrogen Production from Glycerol	46
2.5.1	Catalytic Hydrogen Production from Steam Reforming of Glycerol	46
2.5.1.1	Noble Metal Catalysts	46
2.5.1.2	Non-noble Metal Catalysts	47
2.5.2	Catalytic Hydrogen Production from Aqueous-Phase Reforming of Glycerol	48
2.6	Catalytic Hydrogen Production from Ethylene Glycol	49
2.6.1	Catalytic Hydrogen Production from Steam Reforming of Ethylene Glycol	49
2.6.2	Catalytic Hydrogen Production from Aqueous-Phase Reforming of Ethylene Glycol	50
2.7	Catalytic Hydrogen Production from Sorbitol	51
2.8	Conclusions and Future Outlook	52
	References	52

3 Advances in Fischer–Tropsch Synthesis for the Production of Fuels and Chemicals 57

Liangshu Zhong

3.1	Introduction	57
3.2	Catalyst Development for Fischer–Tropsch Synthesis	59
3.2.1	Fe-Based FTS	59
3.2.2	Co-Based FTS	62
3.3	Selectivity Control for the Production of Hydrocarbon Liquid Fuels	64
3.3.1	Modified FTS Catalysts for Selectivity Control of Liquid Fuels	65
3.3.2	Bifunctional Catalysts for Selectivity Control of Liquid Fuels	65
3.4	Selectivity Control for Production of Chemicals	68
3.4.1	Syngas to Olefins	68
3.4.1.1	Fe-Based FTO	68
3.4.1.2	Co-Based FTO	69
3.4.1.3	Bifunctional Catalysts for Syngas to Olefins	72
3.4.2	Syngas to Aromatics	74
3.4.2.1	STA via Olefins as Intermediates (SOA)	74
3.4.2.2	STA via Methanol/Dimethyl Ether as Intermediates (SMA)	75
3.4.3	Syngas to C ₂₊ Oxygenates	76

- 3.4.3.1 Co₂C-Containing Co-Based Catalyst for Syngas to C₂₊ Oxygenates 78
- 3.4.3.2 Cu-Modified FTS Catalysts 80
- 3.5 Summary and Outlook 82
- References 84

Part II Methane Activation 93

4 Steam and Dry Reforming of Methane 95

José Luis Rico

- 4.1 Introduction 95
- 4.1.1 Steam Reforming of Methane 95
- 4.1.2 Dry Reforming of Methane 96
- 4.1.3 Thermodynamic Analysis of the SRM and DRM Reactions 97
- 4.2 Heterogeneous Catalysts for the SRM 97
- 4.2.1 Ni-Based and Other Catalysts 98
- 4.2.2 Theoretical Studies on the SRM 104
- 4.3 Heterogeneous Catalysts for the DRM 105
- 4.3.1 Noble Metal Catalysts 105
- 4.3.2 Ni-Based Catalysts 106
- 4.3.3 Co-Based and Other Catalysts 114
- 4.3.4 Theoretical Studies on the DRM 118
- 4.4 Comments on Both SRM and DRM Processes 118
- 4.5 Final Remarks 119
- References 119

5 Methane Activation Over Zeolites 129

Meera A. Shah and Russell A. Taylor

- 5.1 Introduction 129
- 5.1.1 The Direct Conversion of Methane 130
- 5.1.2 Introduction to Zeolites 131
- 5.2 Oxidative Coupling of Methane over Zeolite Catalysts 133
- 5.3 Methane Dehydroaromatization (MDA) 135
- 5.4 Metal-Modified Zeolites for dMtM 144
- 5.4.1 Fe-Modified Zeolites 146
- 5.4.2 Cu-Modified Zeolites 149
- 5.4.2.1 Active Sites for Methane Partial Oxidation in Copper-Modified Zeolites 149
- 5.4.2.2 Reaction Mechanism for the Partial Oxidation of Methane over Copper-Modified Zeolites 151
- 5.4.2.3 Alternatives to Stepwise Methanol Production: Isothermal and Direct Catalytic Conversion of Methane to Methanol over Copper-Modified Zeolites 153
- 5.4.2.4 Effect of Framework Topology and Composition on Methane Partial Oxidation over Copper-Modified Zeolites 154

- 5.4.3 Zn-Modified Zeolites 156
- 5.4.3.1 Mechanism of C–H Activation in Zinc-Exchanged Zeolites 157
- 5.4.3.2 Zinc Oxide Clusters in Zeolites 159
- 5.4.3.3 The Role of Brønsted Acid Sites in C–H Activation 160
- 5.4.3.4 Reactivity of Methane with Small Molecules on Zinc-Modified Zeolites 161
- 5.4.4 Other *d*-Block Metals in Zeolites 161
- 5.5 Outlook 164
- References 165

6 The Selective Oxidation of Methane to Oxygenates Using Heterogeneous Catalysts 183

James H. Carter, Nicholas F. Dummer, Ying Kit Chow, Christopher Williams, Ali Nasrallah, David J. Willock, Graham J. Hutchings, and Stuart H. Taylor

- 6.1 Introduction and Historical Context 183
- 6.2 Liquid-Phase Reactions 185
 - 6.2.1 Zeolite Catalysts 185
 - 6.2.2 Noble Metal Catalysts 187
- 6.3 Gas-Phase Reactions 189
 - 6.3.1 Non-zeolite Catalysts 190
 - 6.3.2 Zeolite Catalysts 192
 - 6.3.2.1 Copper as the Active Component 192
 - 6.3.2.2 Iron as the Active Component 194
- 6.4 Conclusions and Outlook 195
- References 196

Part III Alkane Activation 203

7 Catalytic Cracking of Hydrocarbons to Light Olefins 205

Xia Xiao and Zhen Zhao

- 7.1 Background Introduction 205
- 7.2 Reaction Mechanism of Catalytic Cracking over Zeolites 206
 - 7.2.1 Monomolecular or α -Protolytic Cracking Mechanism 206
 - 7.2.2 Bimolecular Cracking Mechanism 208
 - 7.2.3 Monomolecular and Bimolecular Cracking Mechanism 212
- 7.3 Development of Zeolite Catalysts 214
 - 7.3.1 Zeolites with Different Framework Structures 214
 - 7.3.2 Adjustment of Acid Properties of ZSM-5 Zeolite 220
 - 7.3.2.1 Effect of Si/Al Ratio of ZSM-5 Zeolite 221
 - 7.3.2.2 Tuning of Al Siting and Distribution in ZSM-5 Zeolite 226
 - 7.3.2.3 Modification of ZSM-5 Zeolites with Different Elements 227
 - 7.3.3 Alkaline Metal- and Alkali Earth Metal-Modified ZSM-5 228
 - 7.3.4 Transition Metal-Modified ZSM-5 229

7.3.5	Rare Earth Element-Modified ZSM-5	230
7.3.6	Phosphorus-Modified ZSM-5	232
7.4	Nano-ZSM-5 Zeolite	235
7.5	Hierarchical ZSM-5 Zeolites	242
7.5.1	Mesoporous/Microporous ZSM-5 Zeolites	242
7.5.1.1	Hard Template Method	242
7.5.1.2	Post-treatment Method	243
7.5.1.3	Soft Template Method	243
7.5.1.4	Other Methods	247
7.5.2	Macroporous/Mesoporous/Microporous ZSM-5	249
7.5.3	Composite Zeolites	254
7.6	Outlook	258
	References	260
8	Catalytic Dehydrogenation of Light Alkanes	273
	<i>An-Hui Lu</i>	
8.1	Introduction	273
8.2	Direct Dehydrogenation	274
8.2.1	Commercial Dehydrogenation Processes	274
8.2.1.1	Catofin Process	275
8.2.1.2	Oleflex Process	275
8.2.1.3	ADHO Technology	277
8.2.1.4	Other Processes	277
8.2.2	Direct Alkane Dehydrogenation Catalysts	278
8.2.2.1	CrO _x -Based Catalysts	278
8.2.2.2	Pt-Based Catalysts	281
8.3	Oxidative Dehydrogenation	285
8.3.1	Transition Metal Oxide and Alkaline-Earth Metal Oxychloride Catalysts	285
8.3.1.1	Vanadium Oxide-Based Catalysts	285
8.3.1.2	MoVTenNbO _x Catalysts	287
8.3.1.3	Nickel Oxide-Based Catalysts	288
8.3.1.4	Alkaline-Earth Metal Oxychloride Catalysts	289
8.3.1.5	Chemical Looping ODH	291
8.3.2	Boron-Based Catalysts	292
8.3.2.1	Development of Boron-Based Catalysts	292
8.3.2.2	Active Sites of Boron-Based Catalysts	297
8.3.2.3	Possible Reaction Pathway	301
8.3.3	Carbon-Based Catalysts	307
8.3.3.1	Development of Carbon-Based Catalysts	307
8.3.3.2	Identification of Active Sites	308
8.3.3.3	Selectivity Control of Olefins	310
8.4	Summary and Outlook	313
	References	315

Part IV Zeolite Catalysis 321

- 9 Zeolites for Sustainable Chemical Transformations 323**
Luke Harvey, Matthew Drewery, Eric Kennedy, and Michael Stockenhuber
- 9.1 Introduction to Zeolites and Zeolite Chemistry 323
 - 9.1.1 Zeolite Chemistry 323
 - 9.1.2 Zeolites as Catalysts 324
 - 9.1.3 Size Discrimination: Molecular Sieves 325
 - 9.1.4 Zeolites as Supports for Metal Catalysts 326
 - 9.1.4.1 Methods of Metal Deposition 326
 - 9.1.5 Metals in the Zeolite Framework 329
 - 9.1.5.1 Methods of Preparation 329
 - 9.2 The Nature of Active Sites and Deactivation of Zeolite-Based Catalysts 332
 - 9.2.1 Active Sites in Zeolite Catalysis 332
 - 9.2.1.1 Acid Sites 333
 - 9.2.1.2 Basic Sites 335
 - 9.2.1.3 Redox Sites in Zeolite Catalysts 337
 - 9.3 Causes of Deactivation in Zeolite Catalysts 338
 - 9.3.1 Poisoning 338
 - 9.3.1.1 Deactivation through Carbonaceous Deposits (Coking) 338
 - 9.3.1.2 Inhibition of Catalyst Activity Due to Water 339
 - 9.3.1.3 Poisoning of Palladium Combustion Catalysts 339
 - 9.3.2 Particle Sintering and Agglomeration 342
 - 9.3.2.1 Particle Agglomeration in Ventilation Air Methane Oxidation Catalysts 342
 - 9.4 Future Directions for Zeolite Catalysis 343
 - References 343
- 10 Methanol to Hydrocarbons 351**
Weili Dai, Liu Yang, Guangjun Wu, Naijia Guan, and Landong Li
- 10.1 Background Introduction 351
 - 10.2 The Direct Mechanism for MTH Reaction 352
 - 10.2.1 The Development and Milestones of the Direct Mechanism 352
 - 10.2.2 The First C—C Bond Formation 353
 - 10.3 The Indirect Reaction Mechanism for MTH Reaction 359
 - 10.3.1 Hydrocarbon Pool Mechanism 359
 - 10.3.2 Dual-Cycle Mechanism 364
 - 10.3.3 The Connection Between the Dual Cycles 367
 - 10.4 Bridging the Direct and Indirect Mechanisms 370
 - 10.5 Zeolite Catalysts for MTH Conversion 375
 - 10.6 Summary and Outlook 379
 - References 380

Part V Carbon Dioxide as C1 Building Block 391**11 Overview on CO₂ Emission and Capture 393***Wanlin Gao and Qiang Wang*

- 11.1 Introduction 393
- 11.2 CO₂ Emission and Related Problems 394
- 11.3 CO₂ Capture Technology 395
 - 11.3.1 Precombustion CO₂ Capture 396
 - 11.3.1.1 Intermediate-Temperature Adsorbents 397
 - 11.3.1.2 High-Temperature Adsorbents 400
 - 11.3.2 Postcombustion CO₂ Capture 405
 - 11.3.2.1 Amine-Based Solvents 406
 - 11.3.2.2 Amine-Functionalized Adsorbents 407
 - 11.3.2.3 MOF-Based Adsorbents 408
 - 11.3.2.4 Zeolite Adsorbents 409
 - 11.3.2.5 Carbon-Based Adsorbent 409
 - 11.3.3 Oxy-Fuel Combustion CO₂ Capture 410
 - 11.3.4 Chemical Looping Combustion 411
 - 11.3.5 Direct Air Capture of CO₂ 413
 - 11.3.6 Carbon Capture, Storage, and Utilization 414
- 11.4 Conclusions 415
- Acknowledgments 416
- References 416

12 CO₂ Reduction to Fuels and Chemicals 425*Jian Sun and Lisheng Guo*

- 12.1 Introduction 425
- 12.2 Methanation of Carbon Dioxide 427
- 12.3 Synthesis of C₂₊ Hydrocarbons 430
 - 12.3.1 Alkenes 430
 - 12.3.2 Liquefied Petroleum Gas (LPG) 434
 - 12.3.3 Liquid Fuels 434
 - 12.3.4 Aromatics 440
 - 12.3.5 Synthesis of Alcohol 442
 - 12.3.6 Synthesis of Other Valuable Chemicals 447
- 12.4 Photocatalytic and Electrocatalytic Conversion of CO₂ into Valuable Fuels or Chemicals 449
- References 450

Part VI Biomass Conversion 459**13 Lipids to Fuels and Chemicals 461***Bolong Li, Arif Ali, Shutao Lei, and Chen Zhao*

- 13.1 Introduction 461

13.2	Lipids to Diesel-Range Hydrocarbons	462
13.2.1	Deoxygenation of Lipids over Supported Metal Sulfide Catalysts	463
13.2.2	Deoxygenation of Lipids over Sulfur-Free Metal Catalysts	465
13.3	Lipids to Jet Fuel Hydrocarbons	474
13.4	Lipids to Alkenes	478
13.4.1	Lipids to Alkenes over Homogeneous Catalysts	479
13.4.2	Lipids to Alkenes over Heterogeneous Catalysts	486
13.5	Lipids to Fatty Alcohols	488
13.5.1	Hydrogenation of Oils	488
13.5.2	Hydrogenation of Esters or Methyl Esters	489
13.5.3	Hydrogenation of Fatty Acids	493
13.6	Summary	494
	References	496

14 Lignin Upgrading 507

Yong Guo and Yanqin Wang

14.1	Introduction	507
14.1.1	Structure of Lignin	508
14.2	Catalytic Depolymerization	513
14.2.1	Acid Catalytic Depolymerization	513
14.2.2	Alkaline Catalytic Depolymerization	518
14.2.3	Reductive Catalytic Depolymerization	521
14.2.4	Oxidative Catalytic Depolymerization	527
14.2.5	Other Catalytic Depolymerization	530
14.3	Upgrading of Monomers to Fuels and Chemicals	532
14.3.1	Upgrading Lignin Monomers to Cycloalkanes	532
14.3.2	Upgrading Lignin Monomers to Aromatic Hydrocarbons	537
14.3.3	Upgrading Lignin Monomers to Phenols	542
14.3.4	Upgrading Lignin Monomers to Other Chemicals	546
14.4	Direct Conversion of Lignin to Fuels and Chemicals	547
14.5	Conclusions and Perspective	549
	References	551

Index 559

Preface

Energy can be defined as the ability to do work. Specifically, energy exists in various forms such as chemical energy, thermal energy, and radiant energy. Moreover, the controllable transformation of one form to another is of great significance for modern civilization. With the development of human society, the demand for energy has been increasing generally each year, and energy and its interconversion have become a highly topical issue. Nowadays, there are growing concerns not only about accessible energy reserves but also about the energy infrastructure necessary to maintain sustainable development of society. The concept of sustainable energy, which represents energy that can meet current demand and not cause harmful repercussions for the future, is increasingly recognized. Sustainable energy depends upon not only its origin but also how it is utilized.

Catalysis is a process in which a catalyst can change, generally increase, the rate of a chemical reaction without being consumed in the process. It has had huge impact on society, and the rapid development of human society is always accompanied by notable breakthroughs in catalysis, for example, the well-known catalytic ammonia synthesis, catalytic polymerization, and catalytic cracking processes. Catalysis has an indispensable role in industrial production. It is involved in about 90% of chemical processes and the manufacture of over 60% of industrial products.

Catalysis is closely related to energy. In a general catalytic process, a chemical reaction can proceed much faster than that in the absence of a catalyst, and therefore, less energy may be consumed. More intuitively, catalysis can directly participate in the energy transformation processes, for example, converting thermal energy to chemical energy via thermal catalysis, converting photo energy to chemical energy via photocatalysis, and converting electrical energy to chemical energy via electrocatalysis. A key issue in energy transformation is efficiency, and catalysis undoubtedly plays an essential role in promoting the energy efficiency for more sustainable development. It is well known that the energy structure for society is undergoing distinct changes: i.e. the proportion of traditional energy sources like petroleum and coal applied is gradually declining, the proportion of greener energy is gradually increasing, and, correspondingly, the proportion of sustainable energy is gradually increasing. However, society presently must rely on the traditional fossil energy sources of petroleum (~32%), coal (~27%), and natural gas (~24%). Improvements in the transformation of fossil energy or resources via catalysis

can make a significant contribution to modern requirements. On the other hand, the direct generation of sustainable energy from renewable resources via the development of routes involving heterogeneous catalysis might provide a possible solution to the global energy challenges.

Under such circumstances, it is meaningful and desirable to summarize current research progress in heterogeneous catalysis for sustainable energy. Related to this, this book provides a summary relating to the fundamental science of heterogeneous catalysis and sustainable energy, and it is timely to encourage further research activity in this highly topical research field. In this book, two different aspects are summarized, namely, i) the more efficient transformation of fossil resources using heterogeneous catalysis as a tool and ii) the exploitation of renewable energy through heterogeneous catalysis. Specifically, aspects related to hydrogen energy, methane activation, alkane activation, zeolite catalysis, the application of carbon dioxide as building block, and biomass conversion have been included. The authors of the various chapters included in this book are all active researchers in the field of heterogeneous catalysis and sustainable energy. Authors from around the world, including China, the United Kingdom, Australia, Mexico, and Singapore, have contributed.

Nankai University and
Glasgow University
October, 2021

By *Landong Li and Justin S. J. Hargreaves*

Part I

Hydrogen Economy

1

Catalytic Hydrogen Production

Xingyuan Gao and Sibudjing Kawi

National University of Singapore, Department of Chemical and Biomolecular Engineering, 4 Engineering Drive 4, 117585 Singapore, Singapore

1.1 Introduction

Currently and in the near future, fossil fuels are/will be the major source of hydrogen production [1, 2]. As shown in Figure 1.1, almost all the industrial manufacturing processes for hydrogen rely on fossil fuels directly or indirectly [1]. Among the fossil fuels like coal, heavy hydrocarbons, and natural gas, methane is mostly studied due to its high abundance in the world, such as in the United States and Malaysia [4–8]. On the other hand, around 48% of hydrogen gas is generated from natural gas [9–11]. Moreover, methane is easy to handle and has a high H/C ratio [12]. Therefore, we focus on the thermocatalytic conversion of methane first in this part, followed by the conversion of other fossil fuels to produce hydrogen gas.

1.1.1 Thermocatalytic Decomposition of Methane

Only hydrogen gas and carbon are produced in the thermal decomposition of hydrocarbons. This CO-free process is promising for industry [13, 14]. As the major component of hydrocarbons, methane has drawn much interest in the recent years in the production of hydrogen gas via thermal decomposition. The reaction mechanisms are shown below [9]. Initially, methane is chemisorbed on the exposed face of catalyst crystals; secondly, C—H bonds are broken in gaseous methane molecules to produce methyl groups and hydrogen atoms, followed by stepwise dissociations to generate CH_x and more hydrogen atoms; thirdly, two hydrogen atoms combine to generate hydrogen molecules, which are released in gaseous form; fourthly, atomic carbon aggregates and diffuses onto the surface of catalyst particles; fifthly, nucleation and growth of carbon filaments occur in the trailing face of catalyst particles.

Among several methane cracking technologies like plasma, pyrolytic, thermocatalytic, and photocatalytic routes, we focus on thermocatalytic decomposition due to the simultaneous formation of carbon nanofibers or carbon nanotubes

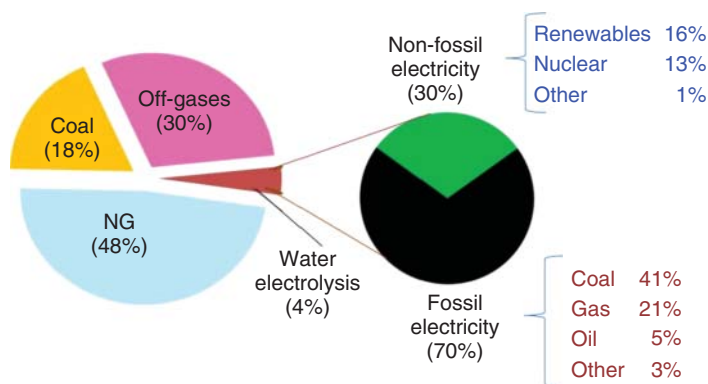


Figure 1.1 The major sources of the industrial hydrogen manufacturing. Source: Reproduced with permission: © 2007, International Energy Agency [3].

that can be potentially used in various applications [14, 15]. Because of the very inactive C—H bond in methane molecules, the activation energy is high, and the reaction is strongly endothermic [16]. Therefore, catalysts are necessary to lower the reaction temperatures and promote the kinetics, including metal- and carbon-based catalysts [1].

1.1.1.1 Metal Catalysts

Since the 1960s, transition metals (Ni, Fe, Co) have been extensively studied and show good catalytic performance in methane decomposition, which occurs at 500–800 °C, much lower than 1200 °C required without a catalyst [17–20]. However, the industrialization of this catalytic system is impeded due to the carbon deposits covering the active sites, leading to rapid deactivation [16, 21]. Modifications have been made to improve the reactivity and stability of transition metal-based catalysts using other transition metals and rare earth metals [22–26].

Bayat et al. [22] studied the Ni–Fe alloy derived from the reduction of the spinel NiFe_2O_4 phase. Below 650 °C, the addition of Fe inhibited the encapsulation of carbon by facilitating the carbon diffusion. However, the active sites become fewer with increasing Fe content due to the lower degree of reducibility. To offset the negative effect of Fe, Bayat et al. [23] doped Cu into the Ni–Fe alloy to enhance the methane adsorption and Ni dispersion on alumina. The optimal ratio of Ni/Fe/Cu was 5 : 1 : 1.

Instead of adding Fe, Lua and Wang [24] doped Co into Ni–Cu to form a tri-metallic alloy. Since Co possesses a high melting point, the quasi-liquid phenomenon occurring between 650 and 775 °C was effectively inhibited, leading to enhanced stability. However, phase separation may be an issue with the further addition of Co. Following this work, a series of catalysts comprising Co and W in different ratios were developed [25]. When Co/W equaled 4 : 1, hydrogen gas and multiwall carbon nanotubes were simultaneously produced, showing the highest conversion of methane. It was found that non-interacted Co_3O_4 was responsible for the superior catalytic performance.

Besides doping of transition metals, a series of rare earth metals were added to Ni to form bimetallic catalysts. Among the additives La, Sr, Nd, Pr, Y, and Sm, Ni–La

Table 1.1 Summary of metal catalysts in methane decomposition.

Catalyst	Conditions	Findings	References
Ni-Fe/Al ₂ O ₃	700 °C for 3 h; 30 vol% CH ₄ and 70 vol% N ₂ .	Fe inhibited the encapsulation of carbon by facilitating the carbon diffusion	[22]
Ni-Fe-Cu/Al ₂ O ₃	700 °C for 3 h; 30 vol% CH ₄ and 70 vol% N ₂ .	Cu enhanced methane adsorption and improved the reducibility and nickel dispersion	[23]
Ni-Co-Cu	500–850 °C; 20 vol% CH ₄ and 80 vol% N ₂ .	The high melting point of Co inhibited the quasi-liquid phenomenon, leading to an enhanced stability	[24]
Co-W/MgO	700 °C; CH ₄ at a flow rate of 50 sccm.	When Co/W equaled to 4 : 1; non-interacted Co ₃ O ₄ was responsible for the highest conversion of methane	[25]
Ni-La-Si	300~750 °C; CH ₄ at a flow rate of 10 ml min ⁻¹	The high activity and low solid carbon formation were attributed to the good thermal stability and small Ni particle size	[26]

exhibited the highest activity and lowest solid carbon formation due to their good thermal stability and small Ni particle size [26] (Table 1.1).

1.1.1.2 Carbon Catalysts

Due to the low cost, resistance to sulfur, and temperature, various carbon materials have been studied as alternatives to transition metals in methane decomposition [1, 16], including active carbon particles [27–30], ordered mesoporous carbons [31, 32], carbon black particles [33], and commercial carbon materials [34]. However, gradual deactivation occurred on carbon catalysts resulting from the coverage of inactive turbostratic carbon. To alleviate this issue, Muradov et al. [35] prolonged methane decomposition by generating active carbon aerosols continuously in a non-thermal plasma device. Besides, Dufour et al. [36] discovered that the addition of small amounts of oxidizing agents like oxygen, CO₂, and steam in the feedstock could effectively enhance the sustainability. Furthermore, the gaseous form of carbon particles derived from partial gasification could inhibit the deactivation of catalyst in a fluid state and cyclic process between the reactor and heater [37].

1.1.2 Partial Oxidation of Methane

Partial oxidation of methane (POM) has drawn much attention recently due to the compactness, good response time, and lower sensitivity to the type of fuels. In the

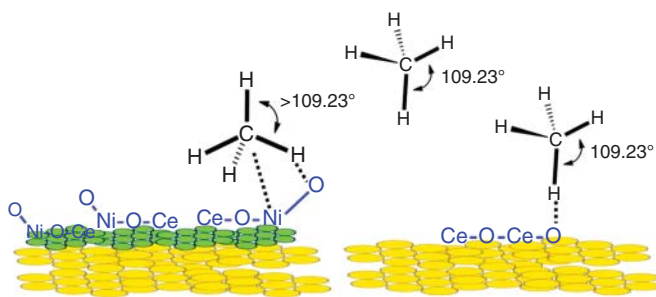
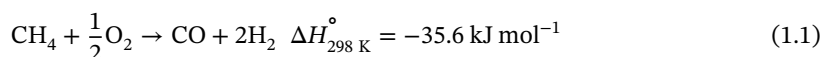


Figure 1.2 Schematic representation of Ni/CeO₂ and CeO₂ surface having surface defects with under coordinated oxygen atoms. Source: Reproduced with permission from Pal et al. [40]; © 2015, American Chemical Society.

presence of oxygen, POM is considered as a fast and highly exothermic reaction to produce syngas as shown in Eq. (1.1) [38]:



The reaction can occur at a very high temperature without catalysts. However, the use of catalysts can lower the reaction temperature greatly that saves the energy input. The commonly studied catalysts for POM include transition metals, noble metals, and perovskites as shown in Table 1.2.

Amongst the transition metals, Ni with different supports is widely applied in POM. Pantaleo et al. [39] compared the catalytic performance of CeO₂ and La₂O₃ single oxide supports and CeO₂-La₂O₃ mixed oxide supports prepared by wet impregnation and coprecipitation. Interestingly, coke only deposited on the single oxide supported catalysts. The enhanced anti-coking property of mixed oxide supported catalyst was attributed to the formation of a series of Ni-La₂O₃ species with different oxidation states of Ni. Besides, in another study regarding Ni/CeO₂ [40], the surface and point defects with undercoordinated oxygen atoms in CeO₂ originating from the formation of O-Ni-O-Ce superstructures promoted the activation of C—H bonds (Figure 1.2). In addition to Ni-based catalysts, Co/ZrO₂ exhibited a very high conversion of methane and selectivity to hydrogen gas, out-performing many other catalysts [41].

Noble metals are also used in POM. A comparison among Pt, Pd, and bimetallic catalysts was conducted by Abbasi et al. [42]. It was found that Pd performed the best in this comparison, followed by the mixture and Pt alone. On the other hand, supports can also affect the performance of Rh-based catalysts [43]. Due to the oxygen spillover from Ce_{0.5}Zr_{0.5}O₂, Rh was easily reoxidized and lost active sites; however, this spillover effect could be alleviated by Al₂O₃.

Perovskite structures present superior anti-coking properties due to the reaction of carbon deposits and oxygen species derived from the structure [60]. Sr_{0.8}Ni_{0.2}ZrO₃ exhibited a highly stable conversion of methane at 900 °C under a reducing atmosphere [44]. Similarly, LaGa_{0.65}Mg_{0.15}Ni_{0.2}O₃ achieved 81% conversion of methane and 100% selectivity to hydrogen gas at 900 °C. This excellent catalytic property may be attributed to the existence of La₂O₃ and La₂O₂Co₃ besides the perovskite structure [45].

Table 1.2 Summary of catalysts in partial oxidation of methane.

Catalyst	Conditions	Findings	References.
Ni/CeO ₂ -La ₂ O ₃	700 °C; WHSV = 60 000; O/C = 0.5	Over 90% methane conversion; the formation of a series of Ni-La ₂ O ₃ species with different oxidation states of Ni inhibited cokes	[39]
Ni/CeO ₂	750 °C; WHSV = 50 000; O/C = 0.5	Over 85% methane conversion and 65% H ₂ selectivity; the surface and point defects originated from the formation of O-Ni-O-Ce structures activated the C-H bonds	[40]
Co/ZrO ₂	800 °C; WHSV = 60 000; O/C = 0.5	Co/ZrO ₂ exhibited 100% conversion of methane and 98.1% selectivity to hydrogen gas	[41]
Pd/γ-Al ₂ O ₃	650 °C; WHSV = 38 400; O/C = 2	Pd performed the best (nearly 100%), followed by Pt-Pd and Pt alone	[42]
Rh/Al ₂ O ₃ and Rh/Ce _{0.5} Zr _{0.5} O ₂	600 °C; WHSV = 252 000; O/C = 2	Rh was easily reoxidized by oxygen spillover in Ce _{0.5} Zr _{0.5} O ₂ ; this spillover effect could be alleviated by Al ₂ O ₃ , maintaining 60% methane conversion for 10 h	[43]
Sr _{0.8} Ni _{0.2} ZrO ₃	900 °C; WHSV = 66 000; O/C = 0.5	Over 94% methane conversion; a highly stable conversion of methane at 900 °C under reducing environment	[44]
LaGa _{0.65} Mg _{0.15} Ni _{0.20} O _{3-δ}	900 °C; WHSV = 3300; O/C = 0.5	81.2% methane conversion and 100% H ₂ selectivity were attributed to the existence of La ₂ O ₃ and La ₂ O ₂ CO ₃ besides the perovskite structure	[45]
Pt-NiO/Al ₂ O ₃	800 °C; WHSV = 7200; O/C = 0.5	91.8% methane conversion and 98.4% H ₂ selectivity; Ni reduction was promoted by Pt	[46]
Co/Al ₂ O ₃	850 °C; WHSV = 60 000; O/C = 0.5	95% methane conversion and 93.6% H ₂ selectivity were attributed to the formation of Co ₃ O ₄ as the major phase after 500 °C calcination	[47]
Ni/12CaO·7Al ₂ O ₃	800 °C; WHSV = 30 000; O/C = 0.5	Over 90% methane conversion and 95% H ₂ selectivity were attributed to the active oxygen ions and high dispersion of Ni.	[48]

Table 1.2 (Continued)

Catalyst	Conditions	Findings	References.
Co/MgO	850 °C; WHSV = 20 000; O/C = 0.5	95% methane conversion, little coke formation, and sintering were attributed to small crystals embedded in the support derived from CoO–MgO solid solution	[49]
Ni/CeO ₂ /Al ₂ O ₃	800 °C; WHSV = 152 432; O/C = 0.5	Low loading of CeO ₂ (1%) generated a highly dispersed CeO ₂ particle, enhancing the reducibility and obtaining 80.3% methane conversion with less carbon deposition	[50]
Ni–Cr/Al ₂ O ₃	700 °C; WHSV = 195 000; O/C = 0.5	85% methane conversion and enhanced stability were realized by the more dispersed Ni particles and surface basicity with addition of Cr	[51]
Ni–Rh/Al ₂ O ₃ –MgO	750 °C; WHSV = 354 044; O/C = 0.5	93% methane conversion and 95% H ₂ selectivity; Rh prevented the oxidation of Ni	[52]
Rh/CeO ₂	700 °C; WHSV = 60 000; O/C = 0.5	The Rh ions in the surface lattice of CeO ₂ were active in POM and obtained 95.2% methane conversion and 92.9% H ₂ selectivity	[53]
Ni/ZrO ₂ @SiO ₂ core shell	750 °C; WHSV = 50 000; O/C = 0.5	Over 90% methane conversion and 75% H ₂ selectivity were obtained with strong coke resistance due to the high oxygen storage capacity and steric hindrance	[54]
Ni/zeolite catalysts	750 °C; WHSV = 90 000; O/C = 0.5	100% methane conversion with strong anti-deactivation ability was attributed to less surface acidity and higher thermal stability	[55]
Ni/TiO ₂	800 °C; WHSV = 4800; O/C = 0.5	86.3% methane conversion and 99.7% H ₂ selectivity were obtained, but serious deactivation was observed, resulting from the NiO and NiTiO ₃ formation	[56]
LaCoO ₃ /γ-Al ₂ O ₃	800 °C; WHSV = 899 550; O/C = 0.25	Over 35% methane conversion and 40% H ₂ selectivity; excellent stability was caused by highly dispersed Co and carbon removal by La ₂ O ₃	[57]

Table 1.2 (Continued)

Catalyst	Conditions	Findings	References.
$\text{La}_{0.08}\text{Sr}_{0.92}\text{Fe}_{0.20}\text{Ti}_{0.80}\text{O}_3$	900 °C; WHSV = 30 000; O/C = 0.5	Over 50% methane conversion and 60% H_2 selectivity; high oxygen vacancy concentration was responsible for the high activity	[58]
$\text{La}_{0.5}\text{Sr}_{0.5}\text{CoO}_3$	850 °C; WHSV = 30 000; O/C = 0.5	Over 70% methane conversion and 75% H_2 selectivity were realized with highly dispersed Co particles in the La_2O_3 and SrO matrix	[59]

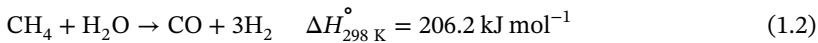
WHSV, weight hour space velocity (unit: $\text{ml h}^{-1} \text{g}_{\text{cat}}^{-1}$); O/C, O_2 -to-carbon ratio.

1.1.3 Catalytic Reforming of Methane

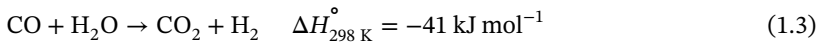
The popular syngas production methods consist of steam reforming of methane (SRM), oxidative steam reforming of methane (OSRM), and dry reforming of methane (DRM). The following will respectively introduce the reaction mechanism, issues to be overcome, and catalytic systems. Kinetic modeling will also be included.

1.1.3.1 Steam Reforming of Methane (SRM)

SRM possesses many advantages, including high hydrogen yield and low cost to obtain hydrogen gas [61, 62]. The reaction equation is shown as below:



Due to the endothermic nature of this reaction, a high reaction temperature is preferred to generate a high yield of H_2 [63]. However, a simultaneous water-gas shift (WGS) reaction occurs, and the CO conversion is inhibited at high temperatures since WGS reaction is exothermic according to Eq. (1.3) [64]:



To solve this issue in industry, a two-reactor system has been adopted to achieve both a high conversion of methane and a high yield of H_2 . In detail, the reactants, methane and steam, are passed through the first reactor operated at 300–450 °C where the reaction is accelerated kinetically and more methane is converted thermodynamically according to Eq. (1.2) in spite of the low conversion of CO according to Eq. (1.3). Afterward, the intermediate products are continuously fed to the second low-temperature reactor (175–250 °C) with a high ratio of steam to convert more CO to form CO_2 and H_2 [65, 66].

To further purify or enhance the yield of hydrogen gas in the final products, CO_2 and H_2 is required to be removed *in situ* respectively by sorbents and selective membranes as shown in Figure 1.3 [67].

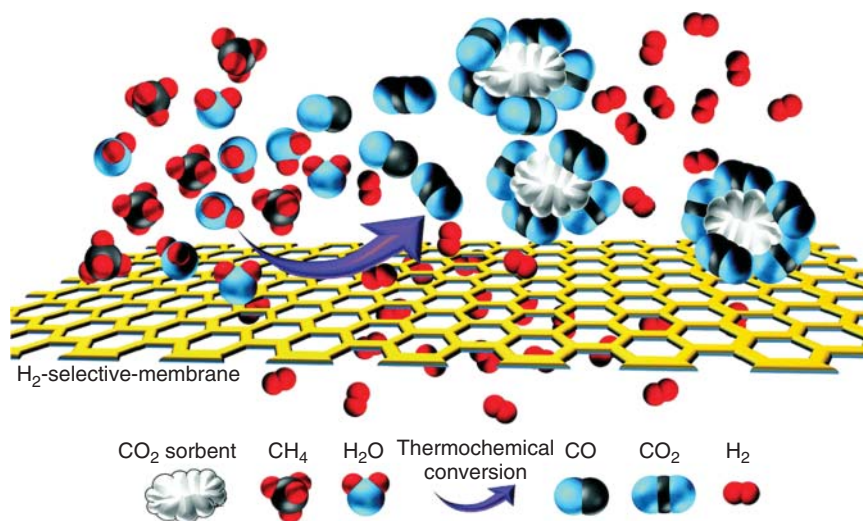


Figure 1.3 Representation of H_2 and CO_2 removal by H_2 -selective membranes and using CO_2 sorbents. Source: Reproduced with permission from Ji et al. [67]; © 2018, The Royal Society of Chemistry.

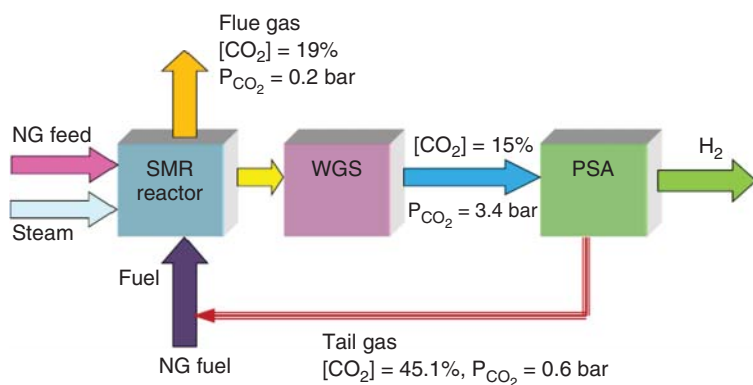


Figure 1.4 Simplified block diagram of a modern SMR plant with major CO_2 containing streams. SMR, steam methane reforming; WGS, water-gas shift reactor; PSA, pressure swing adsorption unit. Source: Reproduced with permission from Muradov [1]; © 2017, Elsevier.

Specifically for CO_2 sorbents, different from the hot potassium carbonate or amine scrubber used about two to three decades ago, pressure swing adsorption (PSA), a physical adsorption technology, is widely adopted in modern SRM plants, achieving an ultrahigh purity of 99.999% for H_2 (shown in Figure 1.4) [1]. In this process, CO_2 is not selectively separated from other gases, but used together with CH_4 and CO to provide heat for the reformer with CO_2 as an exhaust vented out of the reactor system in the end [68].

Besides the design of the reactor system, SRM catalysts should possess the following stringent features: high catalytic stability, high conversion of methane, superior

- methane to methanol with oxygen (dMtM) 144
- methanol
- aqueous-phase reforming of 37–38
 - combined reforming of 37
 - hydrogen production 33–38
 - partial oxidation of 35–36
 - steam reforming of 36–37
- methanol-to-hydrocarbons (MTH)
- direct mechanism
 - development and milestones 352–353
 - first C–C bond formation 353–359
 - dual-cycle mechanism 364–367
 - indirect reaction mechanism 370–375
 - hydrocarbon pool mechanism 359–364
 - solid acidic catalysts 352
 - zeolite catalysts 375–379
- methyl ethyl ether (MEE) 355
- methyl *tert*-butyl ether 184
- methyl trifluoroacetate 189
- MgO-based adsorbents 397–399
- microalgae oil 466, 469, 471, 472
- mixed anhydride system 480
- mixed bifunctional catalysts 44, 45
- molecular layer deposition (MLD) 106
- monomolecular 206, 208, 212
- and bimolecular cracking
 - mechanism 212–214
 - α -protolytic cracking mechanism 206–208
- Monsanto technologies 183
- MoVTeNbO_x mixed metal oxide catalyst 287–288
- n**
- nanostructural engineering 294
- nano ZSM-5 zeolite 235–241
- natural gas 3, 33, 57, 129, 130, 133, 164, 184, 273, 351, 397, 406, 411, 425
- natural mordenite 216
- nickel oxide 288–289
- noble metals 6, 11, 14–16, 19, 21, 23, 24, 35, 36, 38–41, 46–47, 50, 63, 98, 103, 105, 106, 115, 187–189, 191, 281, 327, 340, 428, 429, 445, 465, 474, 522, 532, 536, 538, 539, 542, 550
- non-noble metals 15, 34–37, 40, 47–48, 51, 277, 493, 523, 536, 538, 539, 541
- o**
- olefins, syngas to 68, 72–73
- Oleflex process 275–277
- organic structure directing agents (OSDAs) 133, 259
- oxidative catalytic depolymerization 513, 527–530, 550
- oxidative dehydrogenation of propane (ODHP) 285, 293
- oxygenates 57, 59, 72, 76–84, 96, 158, 161, 183–196, 273, 274, 334, 461, 466, 475, 536
- oxygen, electron density of 433
- p**
- Pacol process 275, 277
- palmitic acid 467, 470
- paraffins 66, 72, 74, 76, 82, 206, 207, 212, 216, 217, 225, 228, 235, 246, 259, 380, 441, 461, 462, 464, 470, 471, 475, 479, 486, 548

- partial oxidation of methane (POM) 5–9, 130, 144–146, 149–151, 156, 162, 185, 191
- partial oxidation of methanol (POM) 34–36
- pentaerythritol (PET) 227
- petrochemical industry 57, 214, 220, 258, 478
- phenols 146, 311, 315, 513, 518, 521, 524, 527, 529, 532, 533, 535, 538–546, 550
- phosphorus-modified ZSM-5 232–235
- photocatalysis 449, 527, 530, 531
- physical adsorbent 410
- physical adsorption technologies 10
- post-synthetic techniques 329–332
- posttreatment method 243
- potassium dititanate ($K_2Ti_2O_5$) 404
- pressure swing adsorption (PSA) unit 10, 397
- propane dehydrogenation (PDH) 274, 279
- propylene 205, 210–212, 214, 216–221, 223, 227–229, 231–233, 235, 237, 242–244, 247, 250, 252, 254, 258, 259, 273, 274, 278, 281–284, 286, 289, 290, 292–297, 301, 305, 307, 311–314, 430, 433, 546
- 4-propylguaiaicol 542, 543, 545
- protolysis 207
- Pt-based catalysts 281
- pyrolysis 129, 210, 513, 530
- r**
- rapeseed oil 464, 488
- rare earth (RE) elements 230
- reductive catalytic depolymerization 521–526
- RE-exchanged Y zeolites (REY) catalysts 230
- s**
- SAPO-34 73, 214, 215, 218, 220, 254, 257, 283, 325, 351, 357, 359, 361, 362, 365, 367, 369, 370, 375, 376, 380, 430, 431, 433
- shale gas 57, 74, 183, 184, 195, 273, 313
- sintering 8, 12, 15, 16, 19, 20, 23, 36, 41, 47, 49, 97, 99, 100, 105–107, 109, 110, 115, 119, 129, 143, 281, 283, 313, 329, 342, 401–404, 413, 429, 430, 467
- soft templating method 243–247
- solid carbon (C_s) 5, 136
- solvent degradation 411
- sorbitol ($C_6H_{14}O_6$) 33, 51–52
- sorption enhanced hydrogen production (SEHP) processes 404
- sorption-enhanced steam methane reforming (SES MR) 103
- spectroscopic techniques 315, 352, 379
- steady-state isotopic transient kinetic analysis (SSITKA) 69
- steam catalytic cracking (SCC) 218
- steam cracking technology 205
- steam reforming of ethanol (ESR) 39–41
- steam reforming of ethylene glycol 49–50
- steam reforming of glycerol (GSR) 46–48
- steam reforming of methane (SRM) 9–13, 95–96

- heterogeneous catalysts 97
 - Ni-based 98–104
 - theoretical studies 104–105
 - thermodynamic analysis 97
 - steam reforming of methanol (SRM) 34, 36–37, 40
 - stearic acid (SA) 465, 466, 468, 471, 473, 477, 481, 495
 - strong metal–support interaction (SMSI) 23, 40, 62, 103, 442, 493
 - structure-directing agent (SDA) 132, 133, 243, 259, 325
 - supported bifunctional catalysts 44–46, 67
 - supported metal sulfide catalysts 461–464
 - supported sulfur-free metal catalysts 461
 - swing adsorption reactor cluster 406
 - synchrotron vacuum ultraviolet photoionization mass spectroscopy (SVUV-PIMS) 307
 - syngas to aromatics (STA)
 - methanol/dimethyl ether 75–76
 - olefins 74–75
 - syngas to C₂₊ oxygenates
 - Co-based catalyst 78–80
 - Cu-modified FTS catalysts 80–82
 - syngas to olefins
 - bifunctional catalysts 72–73
 - Co-based FTO 69–72
 - Fe-based catalysts 68–69
 - synthesis gas 14, 95–97, 129
- t**
- tandem isomerization–decarboxylation process 484
 - temperature-programmed desorption (TPD) 113, 308, 327
 - terephthalic acid (TA) 546, 547
 - tetrapropylammonium hydroxide (TPAOH) 247
 - three-dimensional (3D) printing manufacturing 252
 - titanates, fabrication methods for 403
 - transition metals 4–6, 17, 59, 104, 105, 136, 145, 163, 189, 192, 195, 220, 227, 229–230, 281, 284–286, 290, 314, 326, 334, 403, 411, 445, 484, 491, 550
 - triglycerides 461–465, 473–476, 478, 488, 489
 - two-reactor system 9
- u**
- ultra-dispersed diamond (UDD) 311
- v**
- vanadium oxide-based catalysts 285–286
 - Vaska's complex 483, 484
 - vegetable oils 464, 469, 474, 488
 - ventilation air methane oxidation catalysts 342–343
 - volatile compound emissions 411
- w**
- water–gas shift (WGS) reaction 9, 10, 36, 37, 43, 60, 95, 116, 187, 396, 397, 400, 428, 461, 465
- x**
- X-ray absorption fine structure (XAFS) 60, 99, 116, 139, 150, 342

- X-ray photoelectron spectroscopy (XPS) 35, 106, 116, 139, 297, 308, 543
- Z**
- zeolite acidity 189, 227, 235
- zeolite catalysis
 - active sites
 - acid sites 333–335
 - basic sites 335–337
 - redox sites 337–338
 - deactivation
 - poisoning 338–342
 - sintering 342–343
- zeolites 131–133
 - active sites 332–338
 - as catalysts 324–325
 - chemistry 323–324
 - d*-block metals 161–163
 - deactivation 332–338
 - development 214–235
 - with different framework structures 214–220
 - metal deposition 326–329
 - metal-modified 144–146
 - metal preparation methods
 - direct hydrothermal synthesis 329
 - post-synthetic techniques 329–332
 - methane dehydroaromatization 135–144
 - size discrimination 325–326
 - ZSM-5 zeolite 220–228
- zinc oxide clusters 159–160
- zirconia 36, 99, 280, 543
- Zn-modified zeolites
 - Brønsted acid sites 160–161
 - C–H activation 157–159
 - reactivity, of methane with small molecules 161
 - zinc oxide clusters 159–160
- ZSM-5 zeolite
 - modification
 - alkaline metal- and alkali earth metals 228–229
 - phosphorus-modified 232–235
 - transition metal-modified 229–230
 - Si/Al ratio 221–226
 - tuning of Al siting and distribution 226–227
- ZSM-48 zeolite 217, 218